ChemPubSoc Europe

DOI: 10.1002/chem.201705872

CHEMISTRY A European Journal Full Paper

Perylene Chromophores

Isomerically Pure Star-Shaped Triphenylene–Perylene Hybrids Involving Highly Extended π-Conjugation

Edurne Nuin,[a] Vicent Lloret,[a, b] Konstantin Amsharov,[a] Frank Hauke,[a, b] Gonzalo Abellán,[a, b] and Andreas Hirsch*[a, b]

Abstract: The synthesis and characterization of a new type of a highly conjugated heterocyclic π-chromophore, consisting of a central triphenylene core fused with three perylene monoimide units (star-shaped molecules), is described. By judicious bay functionalization with *tert*-butylphenoxy substituents, aggregation was completely prevented by using 1,1,2,2-tetrachloroethane, allowing for a straightforward purification and, for the very first time, the complete separation of the constitutional isomers by HPLC. Both isomers can be easily distinguished by means of several conventional spectroscopic techniques. Furthermore, we have illustrated the absence of supramolecular aggregates and enhanced processability by noncovalent functionalization of graphene substrates, showing an outstanding homogeneity and demonstrating a different doping behavior in both isomers, making it possible to distinguish them by Raman spectroscopy.

Introduction

Perylenetetracarboxylic diimide (PDI)-based materials have become increasingly attractive owing to their good charge-carrier mobilities, excellent light absorption in the wavelength range of visible light, as well as high thermal, chemical, and photostability.[1–9] Beyond optoelectronics, PDIs have been extensively used in the dispersion and noncovalent functionalization of synthetic carbon allotropes such as carbon nanotubes or graphene and in novel 2D materials.[10–13] Moreover, in the last few years, several efforts have been devoted to the design and synthesis of highly extended heterocyclic π systems with extraordinarily large seas of conjugated π electrons.[14,15] A characteristic feature of this family is the continuous bathochromic shift of the absorption and fluorescence emission bands as a consequence of the extension of the conjugated π system.[1,16–21]

The arrangement of PDI-based molecules can be tailored by supramolecular design, inducing perylene core twisting enforced by bay substituents, by the attachment of trialkoxyphenyl wedges, or by a head-to-tail alignment through hydrogen-bonding interactions.[9,19,22,23] PDIs have been extensively studied as exciting building blocks for the supramolecular construction of aggregates, but when it comes to π-extended PDI-based macromolecules, like n-type disk-shaped molecular systems, the number of studies is very limited. These molecules endowed with C_3 symmetry exhibit appealing spectroscopic effects of interest in highly anisotropic media such as liquid crystals as well as in molecular electronics.[1,3] Usually, disk-shaped molecules containing polycyclic aromatic cores have a strong tendency to aggregation into 1D columns, endowing them with anisotropic charge-transport properties. Along this front, Liu and co-workers developed a PDI-based C_3-symmetric star-shaped molecular skeleton exhibiting good electron mobility with a remarkable charge-transport anisotropy.[24,25] However, these systems strongly aggregate and are almost insoluble in common organic solvents, severely limiting their characterization (e.g., by ^{1}H NMR spectroscopy) and processability. Moreover, as a consequence of the condensation reaction between hexaaminotriphenylene and the corresponding anhydrides, these trimeric molecules are obtained as a statistical mixture of C_s (asymmetric) and C_h (symmetric) constitutional isomers, which, to the best of our knowledge, have never been successfully separated.

Herein, we designed and synthesized a highly extended conjugated star-shaped molecule (Scheme 1) that contains a triphenylene core fused with three bay-functionalized twisted perylene imide imidazole "arms". Although these architectures do not contain long and highly flexible side groups in their imide periphery, they are highly soluble in organic solvents.[26] Moreover, we successfully separated the constitutional isomers

[a] Dr. E. Nuin, V. Lloret, Dr. K. Amsharov, Dr. F. Hauke, Dr. G. Abellán, Prof. Dr. A. Hirsch
Chair of Organic Chemistry II
Friedrich-Alexander-Universität Erlangen-Nürnberg
Henkestr. 42, 91054 Erlangen (Germany)
E-mail: andreas.hirsch@fau.de

[b] V. Lloret, Dr. F. Hauke, Dr. G. Abellán, Prof. Dr. A. Hirsch
Joint Institute of Advanced Materials and Processes
Friedrich-Alexander-Universität Erlangen-Nürnberg
Dr.-Mack-Str. 81, 90762 Fürth (Germany)

Supporting information and the ORCID number(s) for the author(s) of this article can be found under https://doi.org/10.1002/chem.201705872.

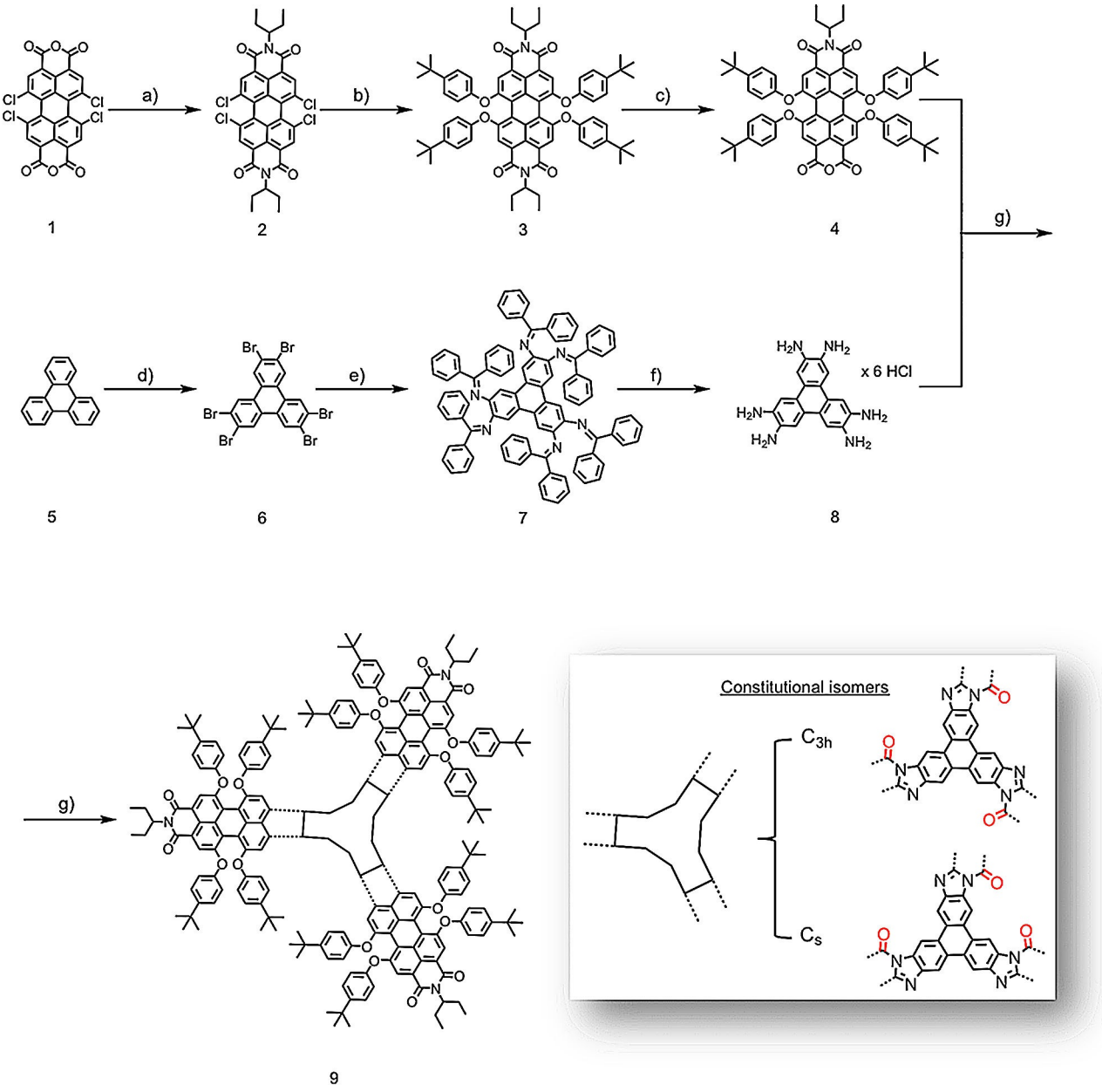

Scheme 1. Synthetic sequence of **9**. Reagents and conditions: a) 3-pentylamine, imidazole, 3 h, 100 °C, N_2; b) 4-*tert*-butylphenol, K_2CO_3, NMP, 16 h, 120 °C; c) KOH, isopropanol/H_2O mixture, 1.5 h, 100 °C; d) Br_2, Fe powder, nitrobenzene, 16 h, 205 °C; e) benzophenone imine, $Pd_2(dba)_3$, *rac*-BINAP, $NaOC(CH_3)_3$, toluene, 16 h, 110 °C, N_2; f) HCl 2 M, THF, 30 min, rt; g) $Zn(OAc)_2$, dry quinoline, 18 h, 180 °C, N_2.

by means of HPLC for the very first time, and differentiated them by using several spectroscopic techniques including NMR and Raman spectroscopy. Further, we have found that these isomer-pure star-shaped molecules form densely packed molecular films on chemical vapor deposited (CVD) graphene with exceptionally high homogeneity.

Results and Discussion

The targeted star-shaped PDI (Scheme 1) was assembled by the condensation of hexaminotriphenylene and perylene monoimide building blocks requiring a multistep synthetic sequence. One of the most common features in highly extended π systems is their tendency to aggregate through π–π stacking, leading to virtually insoluble materials that complicate their purification, characterization, and processing.[27–30] To overcome this hurdles, a widespread approach to obtain soluble aromatic system derivatives is based on the incorporation of bulky solubilizing groups or long alkyl chains in the periphery[19,31] as well as by distortion of their planarity.[28,32] Specifically, the methodology for the synthesis of soluble PDI derivatives is the introduction of branched or long alkyl tails at the imide positions[19,30] and bulky groups like *p*-*tert*-butylphenoxy at the bay positions.[19,20,23,33] As expected, the incorporation of four bulky aryloxy groups attached to the bay positions of each PDI derivative arm lead to a significant distortion of the

planar geometry of the PDI moiety. This is attributed to the repulsive interactions between these sterically encumbered substituents and consequently the PDI twisted out position from the plane, preventing intermolecular π–π stacking.[34–36] Hence, according to Scheme 1, the first part of the synthetic approach started from the 1,6,7,12-tetrachloroperylene-3,4:9,10-tetracarboxylic dianhydride **1**.

Thus, an imidization reaction of **1** with 3-pentylamine in imidazole at 100 °C under N_2 provides, after acidic work-up, the symmetrically *N*,*N*-substituted PDI (**2**) as a red solid with 83% yield. The subsequent nucleophilic substitution of bay chlorine atoms by 4-*tert*-butylphenolate in deaerated NMP at 120 °C yielded tetraphenoxyperylene dimide **3**, which was subsequently partially hydrolyzed to afford the perylene monoimide monoanhydride **4** in 18% yield as a red solid (Figures S1–2 in the Supporting Information).

Once **4** was obtained, the second part of the synthetic procedure consisted of the preparation of the triphenylene core (Scheme 1, center).[37,38] Thus, reaction of triphenylene **5** with Br_2 in nitrobenzene at 205 °C in the presence of Fe powder provides **6** with 85% yield. Then, cross-coupling of the brominated triphenylene with benzophenone imine in toluene catalyzed by $Pd_2(dba)_3$ and using *rac*-BINAP (dba = dibenzylideneacetone, BINAP = (2,2′-bis(diphenylphosphino)-1,1′-binaphthyl)) as the ligand in the presence of $NaOC(CH_3)_3$ afforded **7** as a yellow solid in good yield. The last stage in building the structure of the star-shaped target molecule consisted of linking the individual perylene monoimide monoanhydride **4** with **7**.

Afterwards, deprotection of the amino groups was carried out with 2 M HCl in THF to furnish **8** in 81% yield. Finally, the target molecule was successfully obtained in one step from **4** by reaction with **8** in dry quinoline in the presence of $Zn(OAc)_2$ at 180 °C for 18 h. Under these conditions, final product **9** was isolated as a dark-blue solid in 53% yield (Scheme 1, bottom). As expected, this large π-conjugated architecture exhibits a pronounced aggregation, leading to difficulties in its processing and characterization.[24] Indeed, despite the introduction of the bay-functional *tert*-butoxy moieties—which remarkably improved the solubility of the molecule—the ^{1}H NMR spectrum of **9** recorded in chloroform-d at room temperature showed a significant signal broadening in the aromatic region caused by aggregation. One approach to circumvent this problem is to change the deuterated reference solvent. Along this front, different organic solvents such as [D_6]benzene or [D_2]dichloromethane among others were explored and despite the good solubility of the molecule, the ^{1}H NMR spectra was very broad even at high temperatures (Figure S3 in the Supporting Information). This is due to the interactions with the solvent and the balance of π–π interactions between the extended π systems. However, the strong π–π interactions could be overcome by using 1,1,2,2-[D_2]tetrachloroethane, resulting in sharper NMR signals, indicative of reduced aggregation. Additionally, the behavior of **9** under temperature-dependent ^{1}H NMR spectra was investigated. Figure 1 shows the ^{1}H NMR spectrum of **9** in 1,1,2,2-[D_2]tetrachloroethane measured at 363 K, in which the aromatic proton signals became sharpened and a much better resolution was observed (Figure 1 and Figure S4 in the Supporting Information). Nonetheless, despite all the dilution conditions applied in the spectroscopic measurements, the full characterization based on the analysis of ^{13}C NMR spectroscopy failed to reliably confirm the proposed structure. This may be attributed to the residual aggregation of the molecules in the selected deuterated solvent even at elevated temperatures. Further characterization by high-resolution mass spectrometry measurements was conducted to verify the composition of the final product (Figure 2, inset).

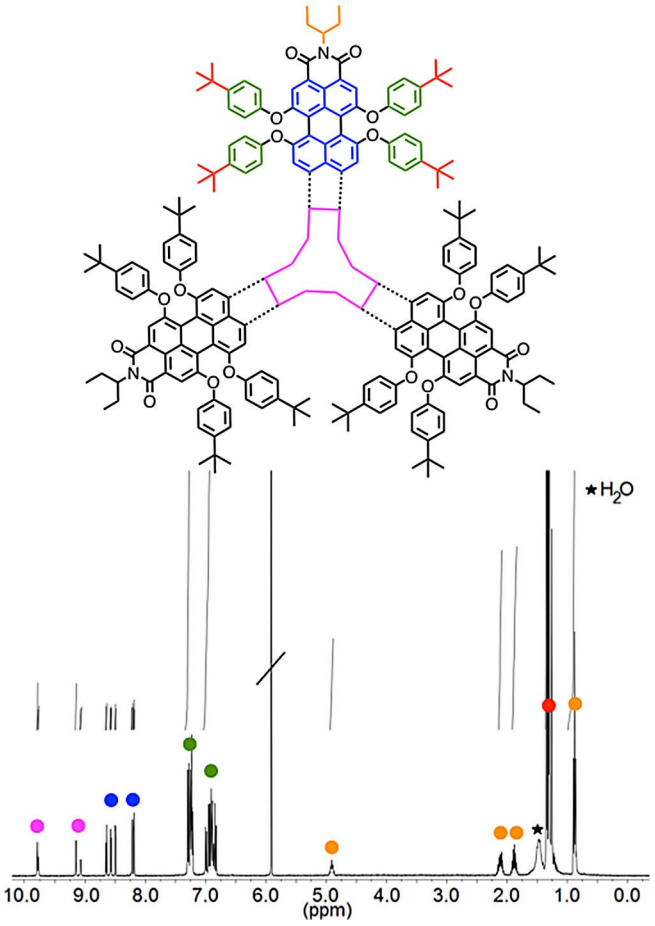

Figure 1. ^{1}H NMR spectrum of compound **9** in 1,1,2,2-[D_2]tetrachloroethane at 363 K.

As can be seen in the inset of Scheme 1, a mixture of all-*trans* (C_{3h} symmetry) and mono-*cis* (C_s symmetry) isomers resulting from the random orientation of the perylene monoimide during the condensation reaction on the central hexaaminotriphenylene of compound **9** was formed. Analysis of the ^{1}H NMR spectrum of the final compound presented in Figure 1 revealed two sets of signals with different intensities in the aromatic region, indicating that **9** was a statistical mixture of the C_{3h} and C_s isomer with yields of approximately 25% and 75%, respectively.

The separation of the isomers of **9** was expected to be very challenging. Indeed, only a few reports on the separation of 1,6- and 1,7-regioisomers of dibromo-, diphenoxy-, and dipyrrolidinyl-substituted perylene diimides derivatives have been reported so far. Typical separation routes consist of crystalliza-

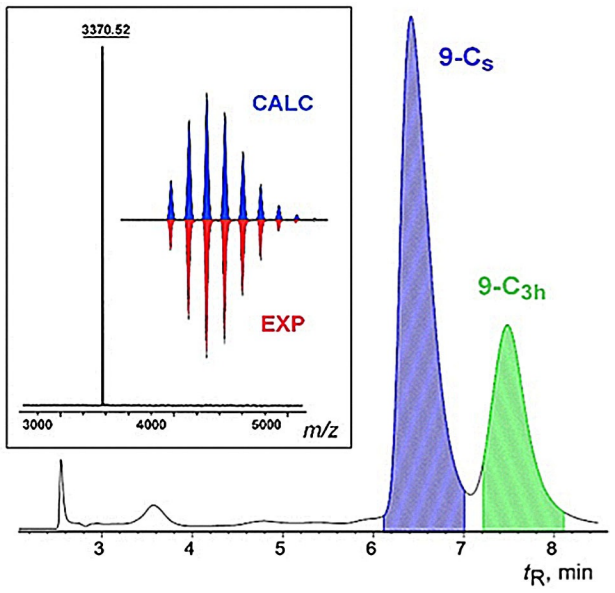

Figure 2. HPLC profile of **9** COSMOSIL-5PBB-R (10×250 mm; eluent CH_2Cl_2/toluene/MeOH 25:35:40; flow rate 5.0 mL min^{-1}; 50 °C; detection 630 nm). The collection regions are highlighted by blue (C_s isomer) and green (C_{3h} isomer). Insert: MALDI mass spectrum of **9** and calculated and experimentally observed isotopic distribution MS pattern.

tion[39] or differences in solubility.[40] In the case of π-extended molecules, the separation of individual isomers appears to be challenging, firstly because of the relatively poor solubility, and secondly owing to very similar chromatographic mobilities.

To face this challenge, high-performance liquid chromatography (HPLC) with a COSMOSIL-5PBB-R semi preparative column (10×250 mm) using a CH_2Cl_2/toluene/MeOH (25:35:40) mixture as the selected mobile phase was employed. Figure 2 shows the HPLC profile of **9**, the peaks of which could be assigned to the C_{3h} and C_s isomer based on their relative intensities. The configurations of the isolated isomers were unambiguously assigned on the basis of ^{1}H NMR analysis of the signals of the perylene core and triphenylene core protons. The ^{1}H NMR spectra of the C_{3h} and C_s isomers of **9** as well as its statistical mixture in 1,1,2,2-[D_2]tetrachloroethane at 363 K are presented in Figure 3 and Figures S5–6 (in the Supporting Information). The ^{1}H NMR of the C_s isomer (Figure 3, top) exhibits six singlets between $\delta = 9.05$–9.85 ppm (bay region of the triphenylene-core). As expected, the 12 protons of the perylene moiety appear in the region $\delta = 8.18$–8.70 ppm (according to the integration), although only 11 singlets can be detected because of the overlap of two signals. Hence, the assignment of the first elution phase at 6.1 min to the isomer with C_s symmetry based on the peaks intensity of the HPLC chromatogram was confirmed. For the minor isomer (second elution phase at 7.2 min) two and four singlets (triphenylene and perylene protons, respectively) were detected, in agreement with the expected C_{3h} symmetry (Figure 3, center). The NMR spectroscopic data recorded for **9** (Figure 3, bottom) exhibited the combination of both isomer signals in the spectrum.

The successful isomers separation was further evident from attenuated total reflectance infrared spectroscopy (ATR-FTIR). Direct comparison of the spectra of the C_{3h} and C_s isomers revealed a rather similar behavior (Figure 4 and Figure S7 in the Supporting Information). In both cases, characteristic stretching vibrations of perylene derivatives at 1694 (1690) cm^{-1} and 1654 (1653) cm^{-1} corresponding to the *N*-imides carbonyl groups were observed for the C_{3h} and C_s isomers, respectively (Figure 4). It is worth noting that, in addition to these vibrations, the FTIR spectrum displayed an additional signal at 1735 cm^{-1}, which is remarkably more intense for the C_s isomer. The lower molecular symmetry increases the molecular dipole moment, which typically enhances the IR active vibrational modes. Thus, the band at 1735 cm^{-1} is assigned to C=O vibration of the asymmetric *N*-imine carbonyl because of the C_3 symmetry breaking in the C_s isomer.[41]

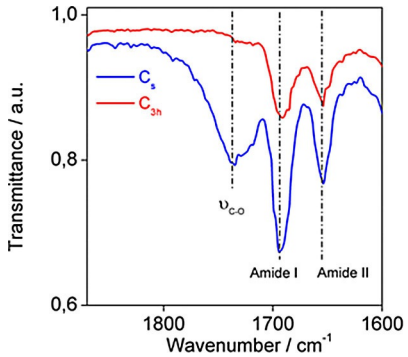

Figure 4. AFT-IR spectra of the C_{3h} (red) and C_s (blue) isomer of **9** in the region between 1600–1850 cm^{-1}.

Steady-state absorption studies in 1,1,2,2-tetrachloroethane at 298 K of the target molecule as well as the different building

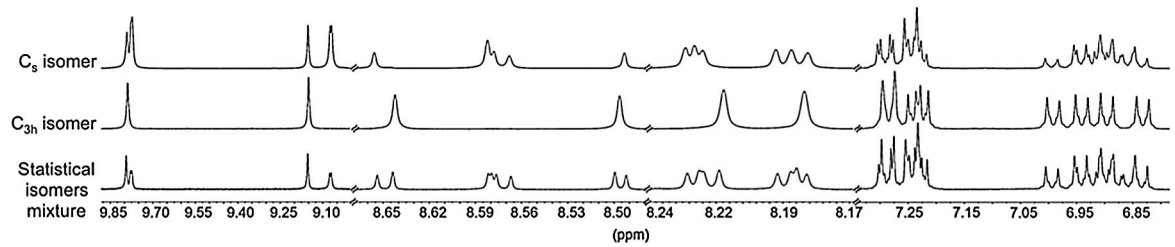

Figure 3. Selected sections of the ^{1}H NMR spectra of the C_{3h} and C_s isomers of **9** as well as its statistical isomers mixture in 1,1,2,2-[D_2]tetrachloroethane at 363 K.

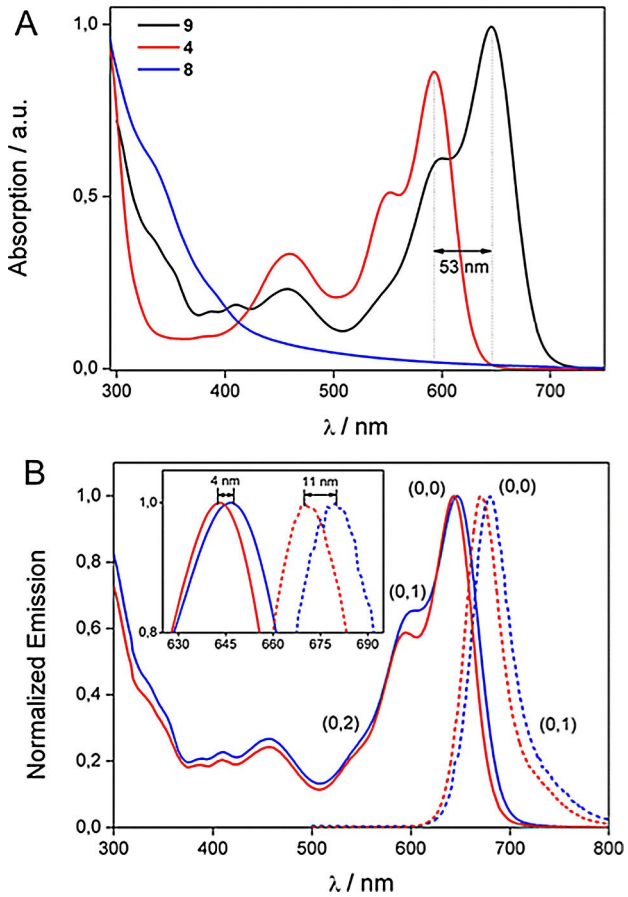

Figure 5. (A) UV/Vis absorption spectra of **9** (black) and the isolated chromophores **4** (red) and **8** (green) in 1,1,2,2-tetrachloroethane at room temperature. The concentration of each sample was 8×10^{-5} M. (B) UV/Vis absorption spectra and steady-state emission spectra of the C_{3h} (red) and C_s (blue) isomers of **9** in 1,1,2,2-tetrachloroethane at room temperature.

blocks were carried out. The UV/Vis absorption spectrum of **4** and **9** is dominated by characteristic π–π* transitions showing a maximum absorption at 592 and 645 nm, respectively (Figure 5).

It is noteworthy to mention that **9** exhibited a bathochromic shift of 53 nm in the absorption maximum, attributed to the extensive conjugation of its 156 π electrons in the star-shaped molecule, higher than those previously observed for benz-bimidazole-bridged perylenes[15] or fused perylene–phthalocyanine hybrids.[14]

This fact indicates an utterly new arrangement of the electron levels from which the optical excitation is facilitated. In the case of tetraryloxy-substituted PDI chromophores, the maximum absorption band indicates strongly allowed electronic $S_0\rightarrow S_1$ transitions, generally found in the 400–600 nm range for these sort of molecules, and is characterized by three well-resolved vibronic peaks.[42–46] The ratio between the (0,0) and (0,1) transitions was remarkably larger than 1.6, indicative of monomeric units in solution for both molecules.[47] The broad absorption behavior of **9** covers a larger part of the UV and visible region (250–750 nm), which is of interest for those applications requiring larger absorption cross sections in the visible region of the electromagnetic spectra (e.g., photovoltaic devices).

When comparing the absorption spectra of the separated C_{3h} and C_s isomers, we observed a shift of approximately 4 nm in the (0,0) peak. The fluorescence emission spectra with a peak maximum at 669 (680) nm for the C_{3h} and C_s isomers, respectively, revealed a mirror-like image of the absorption spectra with a Stokes shift of 26 (22) nm with respect to **4**. Remarkably, a shift of approximately 11 nm between both isomers was detected. The calculated quantum yields were 0.09 ± 0.01 and 0.03 ± 0.01 for the C_{3h} and C_s isomers, respectively. Such a pronounced quenching of the emission has been previously observed for related PDIs endowed with 3,4,5-tridodecyloxyphenyl substituents on the imide N atoms and with four *tert*-butylphenoxy substituents in the bay position.[44]

To further confirm the solubility of **9** and its respective isolated isomers in 1,1,2,2-tetrachloroethane, concentration-dependent UV/Vis experiments were carried out.

Figure S8 (in the Supporting Information) shows the spectra collected in the range of concentration comprising 5×10^{-5}–2×10^{-4} M for both isomers, highlighting the increased processability of these extended aromatic macrocycles. Furthermore, temperature-dependent analysis in the 298–353 K range only revealed slight changes in the absorbance, in excellent agreement with the NMR studies (Figure S9 in the Supporting Information).

At this point, we decided to explore the processability of these pure isomers on surfaces to discover whether these molecules presented supramolecular aggregates or not. Firstly, both isomers were spin-coated at 2000 rpm on SiO_2/Si substrates and thoroughly analyzed by means of optical microscopy, scanning Raman microscopy (SRM), and atomic force microscopy (AFM), which showed an inhomogeneous covering of the surface, with no signatures of specific supramolecular aggregation motifs and the presence of fluorescence in the Raman spectra (Figures S10–11 in the Supporting Information). Moreover, when CVD graphene substrates are used—in which π-aromatic molecules tend to lie with the aromatic cores parallel to the surface, stabilized by van der Waals interactions[48–53]—a very homogeneous fluorescence quenching was detected by Raman spectroscopy in the range of millimeters (Figure 6). It is worth noting that normally it is not possible to measure Raman spectra of fluorescent molecules, however by noncovalently binding to graphene or related 2D materials, a fluorescence quenching of the dye can be obtained as a consequence of an electron/energy transfer.[49,54,55] The homogeneity of the films was characterized by means of SRM on areas of $30\times30\ \mu m^2$, measuring with 1 μm steps (>900 single point spectra) and by using a grating of 1800 grooves mm^{-1} (Figure 6a and Figures S12–13 in the Supporting Information). The isolated isomers of the star-shaped molecules exhibited the characteristic Raman peaks associated with the tetraryloxy-substituted PDI chromophores when resonantly excited at 532 nm in backscattering geometry.[49] As recently reported by Duesberg and co-workers, the ratio between the ν_{Ag} (ca. 1351 cm^{-1}) and the G peak of the graphene substrate can be efficiently used as an estimation of the packing density.[56,57] Indeed, both

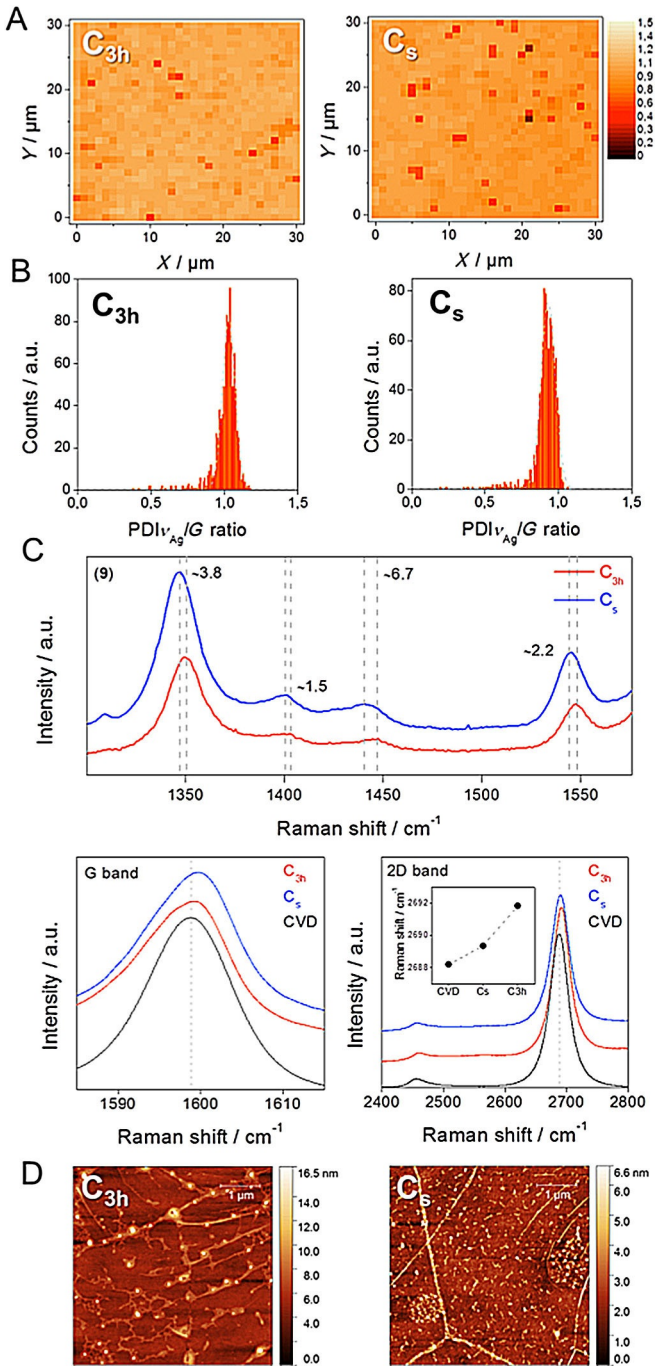

Figure 6. (A) PDI ν_{Ag}/G Raman intensity mappings (measured over a $30\times30\ \mu m^2$ area) of the C_{3h} and C_s isomers deposited on CVD graphene substrates, exhibiting a very high uniformity and homogeneous covering. The color code indicates the PDI ν_{Ag} (ca. 1351 cm^{-1}) and graphene G band intensity ratios. (B) The corresponding PDI ν_{Ag}/G histograms extracted from the statistical analysis of the Raman mappings showing narrow distributions centered at around 1, indicative of a high packing density. (C) Top: Mean Raman spectra of the C_{3h} and C_s isomers highlighting the softening of the Raman modes of the C_s isomer with respect to the C_{3h} isomer, allowing its clear differentiation. Bottom: The characteristic G and 2D graphene Raman modes are shifted as a consequence of the charge transfer (molecular doping). The inset shows the 2D band mode stiffening, which is more intense in the case of the C_{3h} isomer. (D) Topography AFM images of the C_{3h} and C_s isomers (RMS values are 1.6 ± 0.7 and 0.9 ± 0.2, respectively) exhibiting the characteristic corrugations and wrinkles of CVD graphene substrates.

isomers exhibited very homogeneous mean PDI ν_{Ag}/G ratios of 1.03 and 0.93 (full width at half maximum (FWHM) = 0.10 and 0.11) for the C_{3h} and C_s isomers, respectively, indicative of a high packing density (Figure 6b). Interestingly, thanks to the profound quenching of the fluorescence, it was possible to distinguish both isomers when analyzing the PDI-related bands centered at approximately 1351, 1403, 1447, and 1548 cm^{-1}, showing a measurable shift to lower frequencies (mode softening) of all the Raman modes for the C_s with respect to the C_{3h} isomer in the 1.5–6.7 cm^{-1} range (Figure 6c). To the best of our knowledge, this is the first time that constitutional isomers of polycyclic aromatic molecules have been distinguished by Raman spectroscopy. Interestingly, a detailed inspection of the main graphene Raman modes revealed a shift in the position of the graphene bands as a consequence of the interaction with the star-shaped isomers, which is more remarkable in the case of the 2D band. The increase in the Raman modes is indicative of a charge transfer (molecular doping) and is in excellent agreement with previous reports on electron acceptor molecules interactions with graphene.[58,59] This shift to higher frequencies (stiffening) of the G and 2D bands is related to changes in the electronic structure of electron–phonon interactions and suggest a different doping behavior for both isomers, being more intense for the C_{3h} one.[58]

Furthermore, we inspected the samples by atomic force microscopy (AFM), which revealed the presence of characteristic smooth graphene surfaces with the presence of wrinkles, in which thin layers of **9** isomers approximately 3 nm thick were clearly observed, in excellent agreement with related water-soluble PDI thicknesses determined by spectroscopic ellipsometry.[57] The rough mean square values (RMS) of the functionalized surfaces were 1.6 ± 0.7 and 0.9 ± 0.2 for the C_{3h} and C_s isomers, respectively, indicative of a very homogeneous and smooth surface (Figure 6d). Additionally, we have performed Raman mappings with an increased resolution of 200 nm, demonstrating that the covering is completely homogeneous and is not dependent on the corrugations and wrinkles of the graphene substrate (Figures S14–15 in the Supporting Information). Interestingly, the molecules deposited on the graphene substrates were more resilient to washing steps than the ones deposited on SiO_2/Si.

To shine light on the stability of the star-shaped isomers of molecule **9** adsorbed on the graphene surface, we performed temperature-dependent statistical Raman spectroscopy (T-SRS). Figure 7 shows the evolution of the Raman peaks with temperature: surprisingly, the molecules start to desorb from the graphene surface at approximately 475 °C, showing a very high thermal stability. Finally, the pristine monolayer graphene surface was recovered after heating to 500 °C.

These results demonstrate that the star-shaped PDIs **9** can be used to produce homogeneous large areas of noncovalently functionalized graphene, and can be distinguished not only by means of NMR, UV/Vis, fluorescence, or FTIR, but also by using Raman spectroscopy. The more abundant asymmetric isomer (C_s) exhibited the highest absorbance, the more pronounced bathochromic shift in both UV/Vis and fluorescence, as well as a characteristic amide peak in the FTIR spectrum.

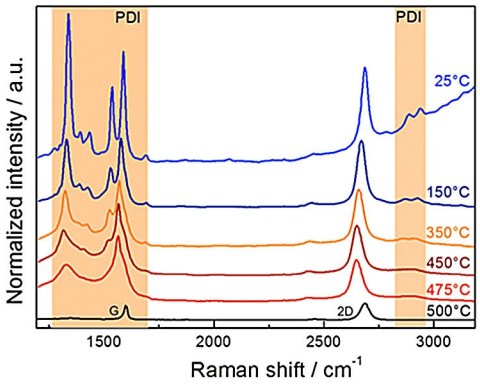

Figure 7. Temperature-dependent statistical Raman spectroscopy (T-SRS) of **9** in the temperature region between 25 and 500 °C. Remarkably, the pristine CVD graphene spectrum can be completely recovered after heating to 500 °C and cooling down to room temperature.

Moreover, both isomers exhibited homogeneous packing on graphene surfaces, exerting measurable G-band mode stiffening. Last but not least, we have been able to differentiate both isomers by Raman spectroscopy by showing a softening of all the Raman modes for the C_s isomer with respect to C_{3h} one.

Conclusion

We have designed and synthesized a highly soluble, very π-extended molecule consisting of a triphenylene core fused with three perylene derivatives yielding a macrocycle endowed with an extended conjugation of 156 π electrons. For the very first time, the respective C_{3h} and C_s isomers have been completely separated by means of HPLC. Both isomers exhibited very high solubility in 1,1,2,2-tetrachloroethane and have been unambiguously characterized and distinguished by means of five spectroscopic techniques, namely ^{1}H NMR, ATR-FTIR, UV/Vis, fluorescence, and Raman spectroscopy. Finally, we explored the self-assembly of these molecules on graphene substrates by optical microscopy, scanning Raman microscopy, and AFM, showing the favorable processability of these star-shaped molecules. This work represents the first example of separation of constitutional isomers of disk-shaped polycyclic aromatic molecules, which can be clearly distinguished by means of several spectroscopic techniques thanks to its enhanced processability, and could be efficiently used for noncovalently functionalized graphene and related 2D materials.[54,48]

Experimental Section

General

Tetrachloroperylene tetracarboxylic acid dianhydride (Cl_4-PTCDA) was purchased from abcr. 3-Pentylamine and bromine were provided from Acros Organics. Imidazole, *tert*-butylphenol, *N*-methyl-2-pyrrolidone (NMP), triphenylene, *rac*-BINAP, benzophenone imine, sodium *tert*-butoxide ($NaOC(CH_3)_3$), zinc acetate ($Zn(OAc)_2$), quinolone, tris(dibenzylideneacetone)dipalladium(0), toluene, tetrahydrofuran (THF), 1,1,2,2-tetrachloroethane, nitrobenzene, and triethylamine (Et_3N) were obtained from Sigma–Aldrich. Potassium carbonate (K_2CO_3) was ordered from SAFC. Acetic acid (HAc), hydrochloric acid (HCl), isopropanol, and potassium hydroxide (KOH) were bought from Grüssing. Biobeads-SX3 was purchased from BIO-RAD. Monolayer CVD graphene films deposited on 300 nm SiO_2/Si substrates were purchased from Graphenea. 2,3,6,7,10,11-Hexabromotriphenylene **6**, *N*,*N*′,*N*″,*N*‴,*N*⁗,*N*⁗′-(triphenylene-2,3,6,7,10,11-hexayl)hexakis(1,1-diphenylmethanimine) **7**, and 2,3,6,7,10,11-hexaaminotriphenylene hydrochloride **8** were synthesized according to reported literature procedures.[37,38]

NMR spectra were recorded with a Bruker Avance 400 (400 MHz) and a Jeol EX 400 (400 MHz) spectrometer. Chemical shifts are given in ppm and referenced to solvent signals. NMR solvents were purchased from VWR or DEUTERO. HRMS were recorded with Bruker microTOF II focus and maXis 4G instruments.

MALDI-TOF HRMS were recorded with an UltrafleXtreme TOF/TOF (Bruker Daltonics). Analytical and preparative HPLC was carried out with a SHIMADZU Prominence system with CBM-20A system controller, LC-20A solvent delivery unit, SIL-20A auto-sampler, CTO-20A column oven, SPD-M20A photodiode array detector, and a DGU-20A on-line degassing unit.

The ATR-FTIR spectra were recorded with a BrukerTensor 27 (ATR or ZnSe plate) spectrometer.

Optical extinction and absorbance was measured with a PerkinElmer Lambda 1050 spectrometer in extinction, in quartz cuvettes with a path length of 0.2 cm.

Fluorescence spectra were acquired with a Horiba Scientific Fluorolog-3 system equipped with a 450 W Xe halogen lamp, double monochromator in excitation (grating 600 lines mm^{-1} blazed at 500 nm) and emission (grating 1200 lines mm^{-1} blazed at 500 nm), and a PMT detector using quartz cuvettes with a path length of 0.2 cm.

Raman spectra were acquired with a LabRam HR Evolution confocal Raman microscope (Horiba) equipped with an automated XYZ table by using 0.80 NA objectives. All measurements were conducted by using an excitation wavelength of 532 nm, with acquisition times of 0.5–2.0 s and a grating of 1800 grooves mm^{-1}. Maps of 30×30 μm were recorded with a step size of 1 μm, giving >1000 single-point spectra.

Temperature-dependent Raman measurements were performed with a Linkam stage THMS 600, equipped with a liquid nitrogen pump (TMS94) for temperature stabilization under a constant flow of nitrogen. The measurements were carried out with a heating rate of 10 K min^{-1}.

Atomic force microscopy (AFM) was carried out by using a Bruker Dimension Icon microscope in tapping mode. The samples were prepared by spin-coating a solution of the separated isomers of **9** at 5000 rpm.

Synthesis of 2

A mixture of Cl_4-PTCDA (3.00 g, 5.63 mmol, 1 equiv), imidazole (9.38 g), and 3-pentylamine (1.76 mL, 14.87 mmol, 2.6 equiv) was heated at reflux at 100 °C under a nitrogen atmosphere for 3 h. After cooling the crude product to room temperature, a solution of HCl in EtOH (5 M, 225 mL) was added, which resulted in the formation of a precipitate. Stirring was continued for a further 12 h. The precipitate was filtered off, washed with water until reaching neutrality, and dried in the oven at 100 °C overnight yielding **2** (3.11 g, 83 %) as a red solid. The desired perylene diimide was used in the next step without further purification. Owing to its low solubility in common organic solvents, ^{1}H NMR and ^{13}C NMR spectra

were found to be coincident with those previously reported.[60] HRMS: calcd for $C_{34}H_{26}Cl_4N_2O_4$: 666.0647 $[M]^+$; found: 666.0642.

Synthesis of 3

Compound **2** (3.11 g, 4.64 mmol, 1 equiv), *tert*-butylphenol (7.66 g, 51.02 mmol, 11 equiv), and K_2CO_3 (8.33 g, 60.29 mmol, 13 equiv) were dissolved in degassed anhydrous NMP (250 mL) and stirred at 120 °C for 16 h under a nitrogen atmosphere. After cooling the mixture to room temperature, an aqueous solution of HCl (2 M, 120 mL) was carefully added. The mixture was stirred for another 4 h. The precipitate formed was filtered, washed with water until reaching neutrality, and dried in the oven at 100 °C overnight yielding **3** (5.00 g, 96%) as a red solid, which was used for the next step without further purification. ^{1}H NMR (400 MHz, $CDCl_3$, 25 °C): $\delta = 0.84$ (t, $J = 7.5$ Hz, 12H, CH_3), 1.27 (s, 36H, CH_3), 1.76–1.88 (m, 4H, CH_2), 2.09–2.20 (m, 4H, CH_2), 4.90–4.98 (m, 2H, CH), 6.82 (d, $J =$ 8.8 Hz, 8H, CH), 7.21 (d, $J = 8.8$ Hz, 8H, CH), 8.19 ppm (s, 4H, CH); ^{13}C NMR (100 MHz, $CDCl_3$): $\delta = 11.3$, 25.1, 31.5, 34.4, 57.6, 119.4, 119.7, 120.3, 126.6, 132.9, 147.2, 152.8, 156.0 ppm; HRMS: *m/z*: calcd for $C_{74}H_{78}N_2O_8$: 1122.4190 $[M]^-$; found: 1122.4192.

Synthesis of 4

KOH (0.88 g, 15.61 mmol, 3.5 equiv) was added dropwise to a solution of **3** (4.99 g, 4.44 mmol, 1 equiv) in a mixture of isopropanol (197 mL) and H_2O (11 mL). The resulting solution was heated at reflux at 100 °C with stirring for 1.5 h. After cooling down the solution, aqueous solutions of HCl (6 M, 230 mL) and AcOH (74 mL) were added. The precipitate was filtered off, washed with water until reaching neutrality, and dried in the oven at 100 °C overnight. After double purification with a plug of silica (CH_2Cl_2/*n*-hexane 34:66), **4** (0.84 g, 18%) was obtained as a pink solid. ^{1}H NMR (400 MHz, $CDCl_3$, 25 °C): $\delta = 0.86$ (t, $J = 7.4$ Hz, 6H, CH_3), 1.30 (s, 36H, CH_3), 1.77–1.91 (m, 2H, CH_2), 2.10–2.22 (m, 2H, CH_2), 4.90–5.00 (m, 1H, CH), 6.83 (d, $J = 8.8$ Hz, 8H, CH), 7.25 (d, $J = 8.8$ Hz, 8H, CH), 8.21 ppm (s, 4H, CH); ^{13}C NMR (100 MHz, $CDCl_3$): $\delta = 11.4$, 25.2, 31.6, 34.6, 57.9, 118.1, 119.6, 119.7, 121.9, 122.0, 122.6, 127.0, 127.1, 133.40, 133.42, 147.9, 148.0, 152.8, 152.9, 156.0, 157.0, 160.4 ppm; HRMS: *m/z* calcd for $C_{69}H_{67}NO_9$: 1055.2710 $[M]^+$; found: 1055.2711.

Synthesis of 9

Et_3N (0.07 mL, 0.52 mmol, 9 equiv) was added dropwise to a suspension of **8** (30.88 mg, 0.06 mmol, 1 equiv) in dry quinoline (6.20 mL) at room temperature under N_2. The resulting mixture was stirred for 30 min and the excess Et_3N was removed under vacuum. Then, **4** (0.20 g, 0.19 mmol, 3.3 equiv) and dry $Zn(OAc)_2$ (47.46 mg, 0.26 mmol, 4.5 equiv) were added and the reaction was heated to 180 °C with stirring overnight. Afterwards, the mixture was allowed to cool down to room temperature and an aqueous solution of HCl (2 M, 10 mL) was added dropwise to quench the reaction. After stirring for 30 min at 40 °C, CH_2Cl_2 was added to the suspension and the layers were separated. The combined organic layers were washed with an aqueous solution of HCl (2 M), then brine, and dried over anhydrous magnesium sulfate and concentrated. The residue was dissolved in CH_2Cl_2 and passed through a pad of silica gel. The crude mixture was further purified by size-exclusion chromatography on Biobeads-SX3 by using CH_2Cl_2 as eluent yielding **9** as a dark-blue solid (103.20 mg, 53.22%). The individual isomers of **9** were separated on a COSMOSIL-5PBB-R column (10×250 mm; eluent CH_2Cl_2/toluene/MeOH 25:35:40; flow rate 5.0 mL min^{-1}; 50 °C; detection 630 nm) yielding the C_s isomer (75.64 mg, 73.31%) and the C_{3h} isomer (27.55 mg, 26.80%) as dark-blue solids.

Characterization data

9: ^{1}H NMR (400 MHz, $C_2D_2Cl_4$, 90 °C): $\delta = 0.88$ (dd, $J = 7.6$, 7.6 Hz, 18H, CH_3), 1.28 (s, 40H, 12CH_3 of C_s isomer and 18CH_3 of C_{3h} isomer), 1.30 (s, 13.5H, 6CH_3, C_s isomer), 1.31 (s, 13.5H, 6CH_3, C_s isomer), 1.34 (br. s, 40H, 12CH_3 of C_s isomer and 18CH_3 of C_{3h} isomer), 1.81–1.95 (m, 6H, CH_2), 2.05–2.18 (m, 6H, CH_2), 4.85–4.96 (m, 3H, CH), 6.81–7.03 (m, 24H, CH), 7.20–7.32 (m, 24H, CH), 8.18 (s, 0.75H, 1CH, C_s isomer), 8.18 (s, 0.75H, 3CH, C_{3h} isomer), 8.19 (s, 0.75H, 1CH, C_s isomer), 8.19 (s, 0.75H, 1CH, C_s isomer), 8.21 (s, 0.75H, 3CH, C_{3h} isomer), 8.220 (s, 0.75H, 1CH, C_s isomer), 8.221 (s, 0.75H, 1CH, C_s isomer), 8.23 (s, 0.75H, 1CH, C_s isomer), 8.49 (s, 0.75H, 1CH, C_s isomer), 8.50 (s, 0.75H, 3CH, C_{3h} isomer), 8.57 (s, 0.75H, 1CH, C_s isomer), 8.576 (s, 0.75H, 1CH, C_s isomer), 8.579 (s, 0.75H, 1CH, C_s isomer), 8.582 (s, 0.75H, 1CH, C_s isomer), 8.64 (s, 0.75H, 3CH, C_{3h} isomer), 8.65 (s, 0.75H, 1CH, C_s isomer), 9.07 (s, 0.75H, 1CH, C_s isomer), 9.08 (s, 0.75H, 1CH, C_s isomer), 9.15 (s, 1.50H, 1CH of C_s isomer and 3CH of C_{3h} isomer), 9.77 (s, 0.75H, 1CH, C_s isomer), 9.78 (s, 0.75H, 1CH, C_s isomer), 9.79 ppm (s, 1.50H, 1CH of C_s isomer and 3CH of C_{3h} isomer); HRMS: *m/z* calcd for $C_{225}H_{207}N_9O_{21}$: 3370.5407 $[M]^+$; found: 3370.5401.

9 (C_s): ^{1}H NMR (400 MHz, $C_2D_2Cl_4$, 90 °C): $\delta = 0.877$ (dd, $J = 7.6$, 7.6 Hz, 6H, CH_3), 0.879 (dd, $J = 7.6$, 7.6 Hz, 6H, CH_3), 0.882 (dd, $J =$ 7.6, 7.6 Hz, 6H, CH_3), 1.30 (br. s, 36H, CH_3), 1.31 (s, 18H, CH_3), 1.33 (s, 18H, CH_3), 1.348 (s, 27H, CH_3), 1.351 (s, 9H, CH_3), 1.81–1.95 (m, 6H, CH_2), 2.04–2.19 (m, 6H, CH_2), 4.85–4.96 (m, 3H, CH), 6.81–7.02 (m, 24H, CH), 7.20–7.32 (m, 24H, CH), 8.18 (s, 1H, CH), 8.187 (s, 1H, CH), 8.193 (s, 1H, CH), 8.223 (s, 1H, CH), 8.22 (s, 1H, CH), 8.23 (s, 1H, CH), 8.49 (s, 1H, CH), 8.57 (s, 1H, CH), 8.578 (s, 1H, CH), 8.582 (s, 2H, CH), 8.66 (s, 1H, CH), 9.069 (s, 1H, CH), 9.074 (s, 1H, CH), 9.15 (s, 1H, CH), 9.77 (s, 1H, CH), 9.78 (s, 1H, CH), 9.79 ppm (s, 1H, CH); HRMS: *m/z* calcd for $C_{225}H_{207}N_9O_{21}$: 3370.5407 $[M]^+$; found: 3370.5401.

9 (C_{3h}): ^{1}H NMR (400 MHz, $C_2D_2Cl_4$, 90 °C): $\delta = 0.88$ (dd, $J = 7.6$, 7.6 Hz, 18H, CH_3), 1.30 (s, 54H, CH_3), 1.34 (s, 27H, CH_3), 1.35 (s, 27H, CH_3), 1.81–1.94 (m, 6H, CH_2), 2.04–2.18 (m, 6H, CH_2), 4.91 (tt, $J = 13.1$, 6.3 Hz, 3H, CH), 6.81–7.02 (m, 24H, CH), 7.20–7.31 (m, 24H, CH), 8.18 (s, 3H, CH), 8.21 (s, 3H, CH), 8.50 (s, 3H, CH), 8.64 (s, 3H, CH), 9.10 (s, 3H, CH), 9.79 ppm (s, 3H, CH); HRMS: *m/z* calcd for $C_{225}H_{207}N_9O_{21}$: 3370.5407 $[M]^+$; found: 3370.5401.

Acknowledgments

The authors thank the Deutsche Forschungsgemeinschaft (SFB 953 "Synthetic Carbon Allotropes", projects A1 & A6) for financial support. In addition, the research leading to these results has received partial funding from the European Union Seventh Framework Program under Grant Agreement No. 604391 Graphene Flagship. G.A. thanks the FAU for the Emerging Talents Initiative (ETI) grant, and the support by the Deutsche Forschungsgemeinschaft and FLAG-ERA (AB694/2-1). E.N. thanks the Programm zur Förderung der Chancengleichheit für Frauen in Forschung und Lehre (FFL) "Promoting Equal Opportunities for Women in Research and Teaching" for a postdoctoral fellowship.

Conflict of interest

The authors declare no conflict of interest.

Keywords: graphene · isomers · noncovalent functionalization · perylene · π conjugation

[1] H. Langhals, *Heterocycles* **1995**, *40*, 477 – 500.
[2] B. A. Jones, M. J. Ahrens, M.-H. Yoon, A. Facchetti, T. J. Marks, M. R. Wasielewski, *Angew. Chem. Int. Ed.* **2004**, *43*, 6363 – 6366; *Angew. Chem.* **2004**, *116*, 6523 – 6526.
[3] H. Langhals, *Helv. Chim. Acta* **2005**, *88*, 1309 – 1343.
[4] C. Zafer, C. Karapire, N. Serdar Sariciftci, S. Icli, *Sol. Energy Mater. Sol. Cells* **2005**, *88*, 11 – 21.
[5] B. A. Jones, A. Facchetti, M. R. Wasielewski, T. J. Marks, *J. Am. Chem. Soc.* **2007**, *129*, 15259 – 15278.
[6] A. Morandeira, J. Fortage, T. Edvinsson, L. Le Pleux, E. Blart, G. Boschloo, A. Hagfeldt, L. Hammarström, F. Odobel, *J. Phys. Chem. C* **2008**, *112*, 1721 – 1728.
[7] R. Centore, L. Ricciotti, A. Carella, A. Roviello, M. Causà, M. Barra, F. Ciccullo, A. Cassinese, *Org. Electron.* **2012**, *13*, 2083 – 2093.
[8] H. Langhals, in *Fundamentals of Picoscience* (Ed.: K. Sattler), CRC Press, Boca Raton, US **2013**, p. 705.
[9] F. Würthner, C. R. Saha-Möller, B. Fimmel, S. Ogi, P. Leowanawat, D. Schmidt, *Chem. Rev.* **2016**, *116*, 962 – 1052.
[10] C. Ehli, C. Oelsner, D. M. Guldi, A. Mateo-Alonso, M. Prato, C. Schmidt, C. Backes, F. Hauke, A. Hirsch, *Nat. Chem.* **2009**, *1*, 243 – 249.
[11] C. Backes, C. D. Schmidt, K. Rosenlehner, F. Hauke, J. N. Coleman, A. Hirsch, *Adv. Mater.* **2010**, *22*, 788 – 802.
[12] C. Backes, F. Hauke, A. Hirsch, *Adv. Mater.* **2011**, *23*, 2588 – 2601.
[13] A. Hirsch, J. M. Englert, F. Hauke, *Acc. Chem. Res.* **2013**, *46*, 87 – 96.
[14] J. Schönamsgruber, H. Maid, W. Bauer, A. Hirsch, *Chem. Eur. J.* **2014**, *20*, 16969 – 16979.
[15] J. Schönamsgruber, A. Hirsch, *Eur. J. Org. Chem.* **2015**, *10*, 2167 – 2174.
[16] T. Furuyama, K. Satoh, T. Kushiya, N. Kobayashi, *J. Am. Chem. Soc.* **2014**, *136*, 765 – 776.
[17] Y. Geerts, H. Quante, H. Platz, R. Mahrt, M. Hopmeier, A. Böhm, K. Müllen, *J. Mater. Chem.* **1998**, *8*, 2357 – 2369.
[18] F. O. Holtrup, G. R. J. Müller, H. Quante, S. De Feyter, F. C. De Schryver, K. Müllen, *Chem. Eur. J.* **1997**, *3*, 219 – 225.
[19] H. Langhals, R. Ismael, O. Yürük, *Tetrahedron* **2000**, *56*, 5435 – 5441.
[20] H. Quante, K. Müllen, *Angew. Chem. Int. Ed.* **1995**, *34*, 1323 – 1325; *Angew. Chem.* **1995**, *107*, 1487 – 1489.
[21] S. K. Lee, Y. Zu, A. Herrmann, Y. Geerts, K. Müllen, A. J. Bard, *J. Am. Chem. Soc.* **1999**, *121*, 3513 – 3520.
[22] H. Langhals, S. Demmig, T. Potrawa, *J. Für Prakt. Chem.* **1991**, *333*, 733 – 748.
[23] H. Langhals, O. Krotz, K. Polborn, P. Mayer, *Angew. Chem. Int. Ed.* **2005**, *44*, 2427 – 2428; *Angew. Chem.* **2005**, *117*, 2479 – 2480.
[24] Y. Zhang, D. Hanifi, S. Alvarez, F. Antonio, A. Pun, L. M. Klivansky, A. Hexemer, B. Ma, Y. Liu, *Org. Lett.* **2011**, *13*, 6528 – 6531.
[25] B. Yao, Y. Zhou, X. Ye, R. Wang, J. Zhang, X. Wan, *Org. Lett.* **2017**, *19*, 1990 – 1993.
[26] F. Würthner, *Pure Appl. Chem.* **2006**, *78*, 2341 – 2349.
[27] Ž. Tomović, M. D. Watson, K. Müllen, *Angew. Chem. Int. Ed.* **2004**, *43*, 755 – 758; *Angew. Chem.* **2004**, *116*, 773 – 777.
[28] D. Wasserfallen, M. Kastler, W. Pisula, W. A. Hofer, Y. Fogel, Z. Wang, K. Müllen, *J. Am. Chem. Soc.* **2006**, *128*, 1334 – 1339.
[29] Y. Fogel, M. Kastler, Z. Wang, D. Andrienko, G. J. Bodwell, K. Müllen, *J. Am. Chem. Soc.* **2007**, *129*, 11743 – 11749.
[30] Z. Chen, A. Lohr, C. R. Saha-Möller, F. Würthner, *Chem. Soc. Rev.* **2009**, *38*, 564 – 584.
[31] W. Pisula, M. Kastler, D. Wasserfallen, M. Mondeshki, J. Piris, I. Schnell, K. Müllen, *Chem. Mater.* **2006**, *18*, 3634 – 3640.
[32] Z. Wang, Ž. Tomović, M. Kastler, R. Pretsch, F. Negri, V. Enkelmann, K. Müllen, *J. Am. Chem. Soc.* **2004**, *126*, 7794 – 7795.
[33] H. Quante, P. Schlichting, U. Rohr, Y. Geerts, K. Müllen, *Macromol. Chem. Phys.* **1996**, *197*, 4029 – 4044.
[34] F. Würthner, A. Sautter, J. Schilling, *J. Org. Chem.* **2002**, *67*, 3037 – 3044.
[35] P. Osswald, F. Würthner, *J. Am. Chem. Soc.* **2007**, *129*, 14319 – 14326.
[36] P. Osswald, D. Leusser, D. Stalke, F. Würthner, *Angew. Chem. Int. Ed.* **2005**, *44*, 250 – 253; *Angew. Chem.* **2005**, *117*, 254 – 257.
[37] L. Chen, J. Kim, T. Ishizuka, Y. Honsho, A. Saeki, S. Seki, H. Ihee, D. Jiang, *J. Am. Chem. Soc.* **2009**, *131*, 7287 – 7292.
[38] T. Yatabe, M. A. Harbison, J. D. Brand, M. Wagner, K. Müllen, P. Samorí, J. P. Rabe, *J. Mater. Chem.* **2000**, *10*, 1519 – 1525.
[39] F. Würthner, V. Stepanenko, Z. Chen, C. R. Saha-Möller, N. Kocher, D. Stalke, *J. Org. Chem.* **2004**, *69*, 7933 – 7939.
[40] R. K. Dubey, A. Efimov, H. Lemmetyinen, *Chem. Mater.* **2011**, *23*, 778 – 788.
[41] T. E. Kaiser, H. Wang, V. Stepanenko, F. Würthner, *Angew. Chem. Int. Ed.* **2007**, *46*, 5541 – 5544; *Angew. Chem.* **2007**, *119*, 5637 – 5640.
[42] R. Gvishi, R. Reisfeld, Z. Burshtein, *Chem. Phys. Lett.* **1993**, *213*, 338 – 344.
[43] J. Hofkens, T. Vosch, M. Maus, F. Köhn, M. Cotlet, T. Weil, A. Herrmann, K. Müllen, F. C. De Schryver, *Chem. Phys. Lett.* **2001**, *333*, 255 – 263.
[44] F. Würthner, C. Thalacker, S. Diele, C. Tschierske, *Chem. Eur. J.* **2001**, *7*, 2245 – 2253.
[45] Z. Chen, U. Baumeister, C. Tschierske, F. Würthner, *Chem. Eur. J.* **2007**, *13*, 450 – 465.
[46] X.-Q. Li, X. Zhang, S. Ghosh, F. Würthner, *Chem. Eur. J.* **2008**, *14*, 8074 – 8078.
[47] C. Huang, S. Barlow, S. R. Marder, *J. Org. Chem.* **2011**, *76*, 2386 – 2407.
[48] J. M. Englert, J. Röhrl, C. D. Schmidt, R. Graupner, M. Hundhausen, F. Hauke, A. Hirsch, *Adv. Mater.* **2009**, *21*, 4265 – 4269.
[49] N. V. Kozhemyakina, J. M. Englert, G. Yang, E. Spiecker, C. D. Schmidt, F. Hauke, A. Hirsch, *Adv. Mater.* **2010**, *22*, 5483 – 5487.
[50] S. M. Kozlov, F. Viñes, A. Görling, *Adv. Mater.* **2011**, *23*, 2638 – 2643.
[51] F. G. Brunetti, H. Isla, J. Aragó, E. Ortí, E. M. Pérez, N. Martín, *Chem. Eur. J.* **2013**, *19*, 9843 – 9848.
[52] M. Marcia, C. Vinh, C. Dolle, G. Abellán, J. Schönamsgruber, T. Schunk, B. Butz, E. Spiecker, F. Hauke, A. Hirsch, *Adv. Mater. Interfaces* **2016**, *3*, 1600365.
[53] M. Garrido, J. Calbo, L. Rodríguez-Pérez, J. Aragó, E. Ortí, M. A. Herranz, N. Martín, *Chem. Commun.* **2017**, *53*, 12402 – 12405.
[54] G. Abellán, V. Lloret, U. Mundloch, M. Marcia, C. Neiss, A. Görling, M. Varela, F. Hauke, A. Hirsch, *Angew. Chem. Int. Ed.* **2016**, *55*, 14557 – 14562; *Angew. Chem.* **2016**, *128*, 14777 – 14782.
[55] G. Abellán, P. Ares, S. Wild, E. Nuin, C. Neiss, D. Rodriguez-San Miguel, P. Segovia, C. Gibaja, E. G. Michel, A. Görling, *Angew. Chem. Int. Ed.* **2017**, *56*, 14389 – 14394; *Angew. Chem.* **2017**, *129*, 14581 – 14586.
[56] N. C. Berner, S. Winters, C. Backes, C. Yim, K. C. Dümbgen, I. Kaminska, S. Mackowski, A. A. Cafolla, A. Hirsch, G. S. Duesberg, *Nanoscale* **2015**, *7*, 16337 – 16342.
[57] S. Winters, N. C. Berner, R. Mishra, K. C. Dümbgen, C. Backes, M. Hegner, A. Hirsch, G. S. Duesberg, *Chem. Commun.* **2015**, *51*, 16778 – 16781.
[58] R. Voggu, B. Das, C. S. Rout, C. N. R. Rao, *J. Phys. Condens. Matter* **2008**, *20*, 472204.
[59] H. Liu, Y. Liu, D. Zhu, *J. Mater. Chem.* **2011**, *21*, 3335 – 3345.
[60] K. Mahata, P. D. Frischmann, F. Würthner, *J. Am. Chem. Soc.* **2013**, *135*, 15656 – 15661.

Manuscript received: December 11, 2017
Accepted manuscript online: January 15, 2018
Version of record online: February 27, 2018

